Pharm Res (2012) 29:837–846
DOI 10.1007/s11095-011-0611-6

RESEARCH PAPER

Mesoporous Silicon (PSi) for Sustained Peptide Delivery: Effect of PSi Microparticle Surface Chemistry on Peptide YY3-36 Release

Miia Kovalainen • Juha Mönkäre • Ermei Mäkilä • Jarno Salonen • Vesa-Pekka Lehto • Karl-Heinz Herzig • Kristiina Järvinen

Received: 10 June 2011 / Accepted: 17 October 2011 / Published online: 27 October 2011

ABSTRACT

Purpose To achieve sustained peptide delivery via mesoporous silicon (PSi) microparticles and to evaluate the effects of different surface chemistries on peptide YY3-36 (PYY3-36) delivery.

Methods PYY3-36 was loaded into thermally oxidized (TOPSi), thermally hydrocarbonized (THCPSi) and undecylenic acid treated THCPSi (UnTHCPSi) microparticles with comparable porous properties. *In vitro*, PYY3-36 release was investigated by centrifuge. *In vivo*, PYY3-36 plasma concentrations were analyzed after delivery in microparticles or solution.

Results Achieved loading degrees were high (12.2 – 16.0% w/w). PYY3-36 release was sustained from all microparticles; order of PYY3-36 release was TOPSi > THCPSi > UnTHCPSi both *in vitro* and *in vivo*. In mice, PSi microparticles achieved sustained PYY3-36 release over 4 days, whereas PYY3-36 solution was eliminated in 12 h. *In vitro*, only 27.7, 14.5 and 6.2% of loaded PYY3-36 was released from TOPSi, THCPSi and UnTHCPSi, respectively. Absolute PYY3-36 bioavailabilities were 98, 13, 9 and 38% when delivered subcutaneously in TOPSi, THCPSi, UnTHCPSi and solution, respectively. The results clearly demonstrate improved bioavailability of PYY3-36 via TOPSi and the importance of surface chemistry of PSi on peptide release.

Conclusions PSi represents a promising sustained and tailorable release system for PYY3-36.

KEY WORDS *in vivo* · mesoporous silicon · peptide delivery · pharmacokinetics · PYY3-36

ABBREVIATIONS

PSi	porous silicon
THCPSi	thermally hydrocarbonized porous silicon
TOPSi	thermally oxidized porous silicon
UnTHCPSi	undecylenic acid treated thermally hydrocarbonized porous silicon

Miia Kovalainen and Juha Mönkäre share equal contribution.

Electronic supplementary material The online version of this article (doi:10.1007/s11095-011-0611-6) contains supplementary material, which is available to authorized users.

M. Kovalainen (✉) • J. Mönkäre • K. Järvinen
School of Pharmacy, Pharmaceutical Technology,
Faculty of Health Sciences, University of Eastern Finland
Po Box 1627, 70211 Kuopio, Finland
e-mail: Miia.Kovalainen@uef.fi

E. Mäkilä • J. Salonen
Department of Physics and Astronomy, University of Turku
20014 Turku, Finland

V.-P. Lehto
Faculty of Science and Forestry, Department of Applied Physics
University of Eastern Finland
70211 Kuopio, Finland

K.-H. Herzig
Institute of Biomedicine, Biocenter of Oulu
University of Oulu
90014 Oulu, Finland

K.-H. Herzig
Department of Psychiatry, Kuopio University Hospital
70211 Kuopio, Finland

INTRODUCTION

Recently, porous silicon (PSi) has attracted considerable interest in drug delivery research due to its beneficial properties, such as biodegradability and biocompatibility, as a drug carrier material (1–3). PSi microparticles contain nanosized pores which tremendously increase the effective surface area of the particles. In drug delivery applications, the drug molecules are attached onto the large internal surface area of PSi, which further allows the adsorption and delivery of high drug payloads within the nanopores. Previously, the PSi pore structure and surface chemistry have been shown to affect the nature of drug adsorption, dissolution and release *in vitro* (4–8). PSi has been investigated for its ability to be used in oral delivery of small, traditional drug molecules with the aim being to improve the absorption of poorly soluble drugs, such as indomethacin (5,9). In addition, PSi has potential for cancer chemotherapy applications, for example oxidation triggered delivery of doxorubicin has been investigated *in vitro* (10). Also proteins or peptides, such as human/bovine serum albumin (HSA/BSA), papain and insulin, have been loaded on PSi surfaces with different surface modifications and investigated *in vitro*, including intracellular protein delivery (6–8,11,12). Our recent *in vivo* studies with several different physiological parameters indicated that THCPSi microparticles could sustain the *in vivo* effects of peptides (13,14). Favorably, peptide loading onto PSi does not require stressful procedures, which could damage the molecules leading to their bioinactivation, which has been a problem with various particulate systems (15–17).

Native PSi is unstable and is therefore typically stabilized and depending on the type of application, the PSi surface can be further modified. Partial oxidation of PSi (thermally oxidized PSi, TOPSi) surface under mild temperatures produces a hydrophilic surface with moderate stability, whereas thermal hydrocarbonization of PSi creates more stable, hydrophobic surface covered with hydrocarbons (THCPSi) (1,18). A novel surface chemistry procedure, thermal functionalization of THCPSi with undecylenic acid (UnTHCPSi) produces a moderately hydrophilic surface with hydroxyl groups, which can be easily further modified. As far as we are aware, the pharmacokinetic parameters of peptides after the administration in PSi and the effects of different surface chemistries of PSi on those parameters have not been reported earlier.

Peptide YY (PYY) is an endogenous peptide belonging to the same peptide family as neuropeptide Y (NPY) and pancreatic polypeptide (PP). PYY consists of 36 amino acids and is a gut peptide secreted by enteroendocrine L-cells of the gastrointestinal tract in response to a caloric load (19). It was isolated originally from porcine intestinal and it is able to cross the blood brain barrier through a non-saturable mechanism (20,21). The effects of PYY3-36 on food intake have been investigated in several animal species and also in humans (22,23). In rodents, it has been shown that PYY administration can reduce both food intake and body weight (24). In obese and normal-weight human subjects PYY3-36 has a reducing effect on food intake (25–27). In addition to appetite regulation, PYY3-36 also seems to have a role in fuel substrate partitioning and energy homeostasis (28). Due to these actions; the PYY system has been suggested to be a potential target for the treatment of obesity (29,30).

In attempts to investigate its physiological functions, PYY3-36 has been delivered chronically via osmotic minipumps or infusions using different experimental arrangements in laboratory animals (30,31). However, because of the promising characteristics of PYY in the treatment of obesity, also other suitable delivery systems have been investigated. For example, reversibly PEGylated PYY3-36 has been shown to evoke a prolonged inhibition of food intake in mice (32). In humans, intranasal delivery of PYY3-36 has been tested in obese adults (33). However, the administration frequency was three times per day. Higher doses caused nausea in the test subjects and no statistically significant weight loss was detected with lower doses. A longer lasting clinical trial has also been conducted by Nastech Pharmaceutical Company Inc. (34) using intranasal PYY3-36 with a similar administration frequency as in the previous study. Recently, PYY3-36 has been combined with GLP-1 and the combination was administered orally with a delivery agent SNAC, but elevated plasma concentrations could only be detected for 2 h (23). Since all of these tested delivery systems require repeated administration, a sustained release system would be preferable. Furthermore, a sustained release system could help to overcome the side effects evoked by high doses as well as eliminating the need for frequent administration. Due to the interesting physiological features of PYY3-36 and previous promising results achieved using PSi in peptide delivery (13,14), this peptide was chosen as a model peptide for pharmacokinetic evaluation of PSi formulations. In the present study, the effects of three different surface chemistries of PSi microparticles on peptide delivery properties were investigated both *in vitro* and *in vivo* by using PYY3-36.

MATERIALS AND METHODS

Reagents

The silicon wafers were purchased from Cemat Silicon S.A. (Warsaw, Poland). Ethanol (EtOH, 99.5%) was bought from Altia (Helsinki, Finland). Hydrofluoric acid (HF)

(37% – 39%) was acquired from Merck KGaA (Darmstadt, Germany). The nitrogen (99.999%) and the acetylene (99.6%) gases were bought from AGA (Espoo, Finland). Sodium chloride solution (9 mg/ml) for injections was obtained from B. Braun Melsungen AG (Melsungen, Germany).

Human PYY3-36 (PYY3-36, M_w 4050 g/mol) was prepared by BCN Peptides (Barcelona, Spain). HPLC reagents were acetonitrile (HPLC grade, JT Baker, Deventer, The Netherlands), trifluoroacetic acid (Sigma–Aldrich, St. Louis, MO, USA). pH 7.4, 0.15 M phosphate-buffered saline (PBS, $\mu = 0.167$) was used as a buffer in the *in vitro* release experiments. The buffer contained 8.0 g sodium chloride (JT Baker Deventer, The Netherlands), 0.2 g potassium chloride (Merck KGaA, Darmstadt, Germany), 1.4 g disodium hydrogen phosphate (Merck KGaA, Darmstadt, Germany) and 0.2 g potassium dihydrogen phosphate (Merck KGaA, Darmstadt, Germany) in 1000 ml of deionized water. In addition, bovine serum albumin (BSA, Sigma–Aldrich, St. Louis, MO, USA) (0.1% w/v) was dissolved to the PBS in order to prevent adsorption of PYY3-36 onto the laboratory materials during the *in vitro* experiments (35).

Particle Preparation

The preparation of free standing porous silicon films was described previously (4). The free standing films were ball milled and dry sieved to a 38 – 53 μm size fraction. Aiming to remove any remaining small particles, after the dry sieving the particles were washed on a 38 μm sieve with ethanol. The microparticles were treated with a 1:1 HF: EtOH solution to replace the oxidized surface formed during the milling with a hydrogen termination and dried at 65°C for 1 h.

Thermal hydrocarbonization of PSi microparticles (THCPSi) was performed under continuous N_2/acetylene (1:1) flow as described earlier (18). Treatment at 500°C for 10 min was used in order to maintain partial hydrocarbon terminated and hence a hydrophobic surface.

Functionalization of THCPSi microparticles was made by thermal treatment of the particles in undecylenic acid (UnTHCPSi) at 120°C for 16 h adapting the treatment for the hydrogen terminated PSi introduced by Boukherroub (36). Due to the stressed and unsaturated carbon-carbon bonds existing on the hydrophobic surface of THCPSi particles immediately after the thermal hydrocarbonization, undecylenic acid covalently binds to the THCPSi surface and a treatment efficiency of about 50% can be achieved compared to the hydrogen terminated PSi (Supplementary data S1). This clearly changes the characteristics of the particles, such as their drug loading and release properties, hydrophilicity and zeta potential. In addition, the carboxyl groups attached onto the surface can be used for further functionalization of the particles. Thermal oxidation of PSi microparticles (TOPSi) was performed at 300°C for 2 h in ambient air immediately after milling without any HF treatment. The treated particles were characterized using FTIR measurements (Spectrum BX II, Perkin-Elmer: Supplementary data S2).

Specific surface area of the microparticles was calculated using BET-theory (37). The pore volume, average pore diameter and of the PSi microparticles were calculated from desorption branch of the nitrogen sorption measurements (Tristar 3000, Micromeritics) according to BJH-theory (38). The calculated values for TOPSi revealed an average pore diameter of 10.3 nm, specific surface area of 222 m^2/g and pore volume of 0.76 cm^3/g, for THCPSi; average pore diameter of 11.2 nm, specific surface area of 273 m^2/g and pore volume of 0.94 cm^3/g and for UnTHCPSi; average pore diameter of 10.4 nm, specific surface area of 231 m^2/g and pore volume of 0.76 cm^3/g, which slightly reduce during the surface treatments (Table I).

Particle Loading

PYY3-36 was dissolved in water and the PSi microparticles were immersed in the peptide solution (100 mg/ml) for 1.5 h at room temperature. The loading solution was treated with ultrasound 3 times during the loading to guarantee homogeneity. The particles were filtered from the solution and dried for 3 h at room temperature and then for an additional 30 min in a vacuum. The loading degree was determined by thermogravimetric (TG) analysis (20°C/min, 25°C – 800°C N_2 gas purge 200 ml/min, TGA 7, PerkinElmer) (39). The loading degrees are presented in Table I. Two batches of loaded TOPSi were used in the experiments. Possible interactions between the peptide and the different PSi surface chemistries were studied with attenuated total reflectance (ATR)-FTIR spectroscopy as shown in Fig. 1.

In Vitro Release

Approximately 2 mg of PYY3-36 loaded TOPSi, THCPSi or UnTHCPSi microparticles (containing 293, 250 and 347 μg PYY3-36 in TOPSi, THCPSi and UnTHCPSi, respectively) were suspended in 1.5 ml of pre-warmed 0.15 M PBS buffer containing 0.1% w/v BSA (pH 7.4, $\mu = 0.167$, +37°C) in microcentrifuge tubes. These tubes were placed in a water bath shaker (Grant OLS200, Cambridge, UK) with orbital shaking at a frequency of 120 strokes/min at +37°C. At pre-determined time intervals, the tubes were centrifuged for 2 min (13,000 rpm, 17,000*g*, Heraues Biofuge Fresco, Osterode, Germany), and supernatants were collected for the HPLC analysis of PYY3-36 concentrations. The microparticles

Table I The Characteristics of PSi Microparticles (38–53 μm) and PYY3-36 Release Behavior *In Vitro* and *In Vivo*

PSi type	Pore diameter (nm)	Specific surface area (m^2/g)	Loading degree (% w/w)	Load ($\mu mol/m^2$)	Pore volume (cm^3/g)	*In vitro* released PYY3-36 (%)	PYY3-36 plasma concentration at 1 h (ng/ml)
TOPSi	10.3	222	14.4 –15.2	0.16	0.76	27 ± 2.7	102.7 ± 10
THCPSi	11.2	273	12.2	0.11	0.94	14.5 ± 3	6.1 ± 0.8
UnTHCPSi	10.4	231	16.0	0.17	0.76	6.2 ± 0.6	4.1 ± 0.7

were re-suspended in fresh pre-warmed (+37°C) PBS buffer containing BSA (0.1% w/v) after the supernatant collection. The concentration of water soluble PYY3-36 in buffer was <10% of its maximum solubility (~100 mg/ml in water), and therefore sink conditions were maintained throughout the experiment.

High Performance Liquid Chromatography Analysis of PYY3-36

The samples from PYY3-36 *in vitro* release experiment were analyzed with a Gilson High Performance Liquid Chromatograph. The system consisted of an UV detector (UV/VIS-151), pump (321), autoinjector (234), interface (506 C) and integrator (Unipoint 3.0). The mobile phase was a mixture of acetonitrile (31.5% v/v), water (68.5% v/v) and trifluoroacetic acid (0.1% v/v). The analytical column was a reverse-phase Supelco Discovery Biowide® C-18 column (150×4.0 mm id, particle size 5 µm, Supelco, Bellefonte, PA, USA) which was placed in a column heater during the analysis (+40°C). Samples were diluted appropriately with the mobile solutions before their injection into the HPLC system. The injection volume was 100 µl, flow rate 1 ml/min and PYY3-36 was detected at 200 nm. The concentrations of PYY3-36 were determined by measuring peak areas, which were compared to a linear calibration curve prepared using known standard PYY3-36 concentrations (1–50 µg/ml).

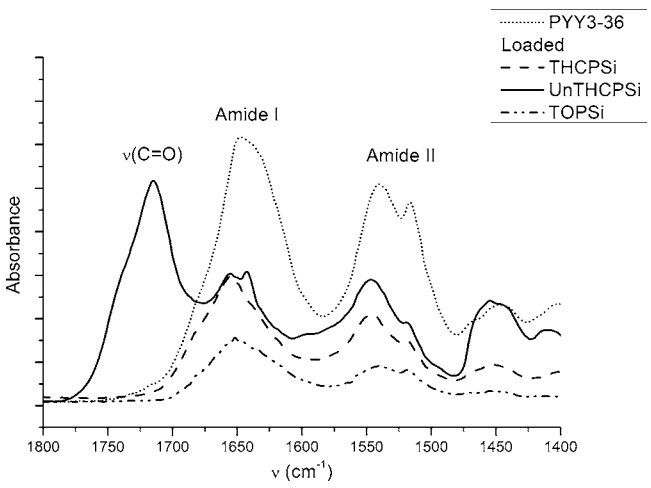

Fig. 1 ATR-FTIR spectra of solid peptide PYY3-36 compared with PYY3-36 loaded THCPSi, UnTHCPSi and TOPSi.

In Vivo Experiment

The BALB/c x DBA2 hybrid mice, for investigating PYY3-36 plasma concentrations after its intravenous and subcutaneous delivery in different formulations, were purchased from Lab Animal Center (Kuopio, Finland) at age of ~8 weeks, weighing 25 – 30 g. They were group housed in a regulated environment; temperature 22±1°C, relative air humidity 55±15% and 12/12 h light/dark cycle with lights on at 7 am. Commercial rodent food (Teklad 2016, Harlan Inc.) and tap water were available *ad libitum* throughout the experiment. The research adhered to the Principles of Laboratory Animal Care. The National Animal Experiment Board of Finland approved the experiments. Procedures were conducted in accordance with the guidelines set by the Finnish Act on Animal Experimentation (62/2006) and European Community Council Directives 86/609/EEC.

The different formulations, containing 20 µg of human PYY3-36 in 1) TOPSi 2) THCPSi 3) UnTHCPSi or 4) 0.9% NaCl-solution were administered subcutaneously in a volume of 200 µl and 5) 20 µg of human PYY3-36 was injected in 0.9% NaCl-solution intravenously through lateral tail vein in a volume of 100 µl. Blood samples were collected from saphenous vein at predetermined time points into heparinized microcapillaries (Drummond Microcaps, Drummond Scientific Co. Broomall, Pa. USA). Plasma was separated by centrifugation (+ 4°C, 3 min, 12000 rpm, Heraues Biofuge Fresco, Osterode Germany) and frozen immediately. Plasma samples were later analyzed using total human PYY3-36 ELISA following the manufacturer's instructions (Millipore Corp., Billerica, MA, USA).

Pharmacokinetic Analysis

Pharmacokinetic parameters for PYY3-36 were determined from plasma concentration-time data by using WinNonlin software (WinNonlin Professional, 5.3, Pharsight Corp, USA) and non-compartmental model for extravascular or bolus intravenous injection in the cases of s.c. or i.v.

administration, respectively, and with uniform weighing. C_{max} and t_{max} –values were obtained directly from the plasma concentration –time data and area under the concentration time curve-value ($AUC_{0\text{-}last}$) was determined by the linear trapezoidal rule and $AUC_{0\text{-}\infty}$-value as follows: $AUC_{0\text{-}last}+C_{last}/K_{e,}$, where C_{last} is the last measured plasma concentration and $K_{e,}$ is the terminal elimination constant. Absolute and relative bioavailabilities were calculated by using $AUC_{0\text{-}\infty}$-values, $F_{absolute}\%=AUC_{(PSi/s.c.\ solution)}/AUC_{i.v.solution}$ x 100%, $F_{relative}\%=AUC_{PSi}/AUC_{s.c.solution}$ x 100%.

Statistical Analysis

Statistical differences of PYY3-36 plasma concentrations were analyzed using 2-way Anova with Bonferroni post test for multiple comparisons. Pharmacokinetic parameters analyzed using 1-way Anova with Bonferroni post-test (GraphPadPrism 4.03 for Windows, GraphPad Software Inc., CA, USA). P-value <0.05 was considered to be statistically significant.

RESULTS

In the present work, PSi microparticles with three different surface chemistries, showing comparable porous properties, were investigated for their abilities to sustain PYY3-36 release *in vitro* and *in vivo*. PYY3-36 was successfully loaded into all the three types of investigated PSi microparticle surfaces and high loading degrees were obtained for the microparticles *i.e.* 12.2, 15.2 and 14.4, 16.0% (w/w) of PYY3-36 in THCPSi, two batches of TOPSi and UnTHCPSi, respectively. Sustained PYY3-36 delivery was achieved with all the microparticles, TOPSi, THCPSi and UnTHCPSi but the surface chemistry strongly affected the PYY3-36 release both *in vitro* and *in vivo*. The characteristics of PSi microparticles and their PYY3-36 releasing behavior *in vitro* and *in vivo* are summarized in Table I.

In Vitro Release

PYY3-36 release from TOPSi, THCPSi and UnTHCPSi microparticles was measured for 14 days *in vitro* (Fig. 2). There was sustained but incomplete PYY3-36 release from all the investigated surfaces and the surface chemistry affected the fraction of peptide released. The highest peptide fraction was released from TOPSi (27.7±2.7% of loaded PYY3-36, mean±SEM) followed by THCPSi (14.5±3.0%) and UnTHCPSi (6.2±0.6%) microparticles, indicating weaker *in vitro* interactions between PYY3-36 and TOPSi than between PYY3-36 and THCPSi or UnTHCPSi. This hypothesis is supported by an ATR-FTIR

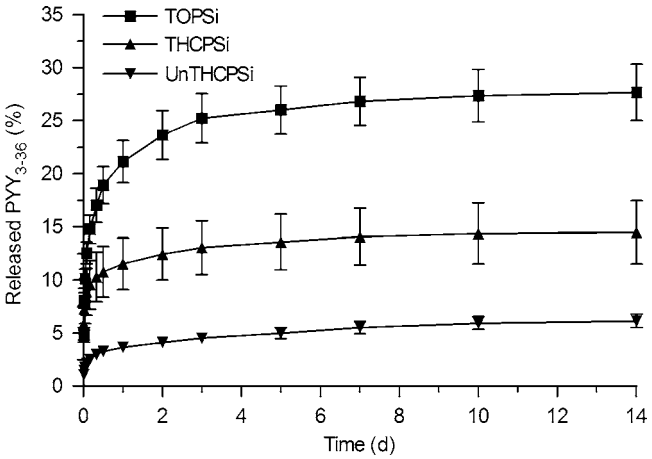

Fig. 2 *In vitro* PYY3-36 release from PSi microparticles with three different surface chemistries (PBS, pH 7.4, 37°C) (Mean ± SEM, $n=4$).

analysis of the peptide loaded PSi. The spectral features of PYY3-36 are superposed on the characteristic spectra of the different PSi surface chemistries after the peptide loading, as presented in Fig. 1. The most notable features are appearance of the broad amide I and II bands centered at 1650 cm^{-1} and 1550 cm^{-1}. Compared with the solid PYY3-36, used as a reference, the adsorption into PSi does not cause major alterations to the FTIR spectra of the peptide. The PYY3-36 loaded TOPSi shows practically no detectable changes in the characteristic amide band regions, for example, the amide I band at 1650 cm^{-1} does not indicate appreciable shift compared with the reference spectra. Similarly, the amide II band appears unchanged. However, The PYY3-36 loaded THCPSi and UnTHCPSi spectra show small changes in both, the amide I and II band regions. In both cases, there appears to be a general shift of 4–5 cm^{-1} towards higher wavenumber. These small shifts are considered to be related to local changes in a particular conformation (40). As the main difference between the PSi surface chemistries is their hydrophilicity, the shift in the amide bands presumably indicates that peptide has a slightly different orientation after the adsorption to the pore wall surface of THCPSi or UnTHCPSi microparticles.

Pharmacokinetics of PYY3-36 After Subcutaneous Delivery via PSi Microparticles in Mice

A dose of 20 μg of PYY3-36 was administered using the differently surface treated PSi microparticles (TOPSi $n=5$, THCPSi $n=6$ and UnTHCPSi $n=6$, s.c.). Subcutaneous ($n=4$) and intravenous ($n=6$) PYY3-36 (dose 20 μg) solutions were studied as controls. First, there was sustained PYY3-36 release from all the microparticles (Fig. 3). When PYY3-36 was injected in a subcutaneous or intravenous solution, the peptide had been eliminated

within 12 h from the plasma (Fig. 3). On the contrary, after administration of the PYY3-36 loaded microparticles, PYY3-36 could be detected in plasma up to 96 h after the injections (Fig. 3). After administration of the PSi formulations, there are many simultaneous pharmacokinetic processes; PYY3-36 release from the PSi, absorption to the blood circulation and elimination. When terminal half-lives ($t_{1/2}$) were calculated for circulating PYY3-36, the results were 7±1 (mean+SEM), 21±2 and 20±1 h after subcutaneous administration of TOPSi, UnTHCPSi and THCPSi, respectively, whereas the half-life of the PYY3-36 solution was a mere ~25 min (Table II). This is evidence for so-called flip-flop pharmacokinetics for PYY3-36 delivery via PSi microparticles since the peptide release from the microparticles controls the detected PYY3-36 plasma concentrations (41).

Secondly, the particle surface chemistry strongly affected the release rate of PYY3-36 and hence modified the pharmacokinetics (Table II). The highest PYY3-36 peak concentration (C_{max}) was obtained for TOPSi being 103± 8 ng/ml, when the corresponding values for THCPSi and UnTHCPSi were 22±6 ng/ml and 13±2 ng/ml, respectively. However, the time when the C_{max} was reached (t_{max}) with TOPSi (51±9 min) was significantly delayed when compared with t_{max} values of THCPSi and UnTHCPSi (11±2 min and 19±8 min, respectively), but not from that of the s.c. solution (26±11 min). PYY3-36 plasma concentrations were significantly higher until 4 h after the administration with TOPSi microparticles compared with THCPSi and UnTHCPSi.

Thirdly, the extent of released fraction of PYY3-36 exhibited the same rank order TOPSi>THCPSi> UnTHCPSi *in vitro* and *in vivo*, but the absorbed fractions were higher *in vivo* than the released fractions *in vitro* (Figs. 2 and 3). The absolute bioavailability of PYY3-36 after administration in TOPSi was 98±16% indicating complete peptide release and absorption from the particles, while the absolute bioavailabilities after PYY3-36 delivery in THCPSi and UnTHCPSi were 13±2 and 9±1%, respectively (Table II). Interestingly, the bioavailability of s.c. PYY3-36 solution was only 38±7%. The relative bioavailabilities, when compared with s.c. solution, of PYY3-36 after administrations in TOPSi, THCPSi and UnTHCPSi were 256±41%, 34±3% and 25±2%, respectively (Table II).

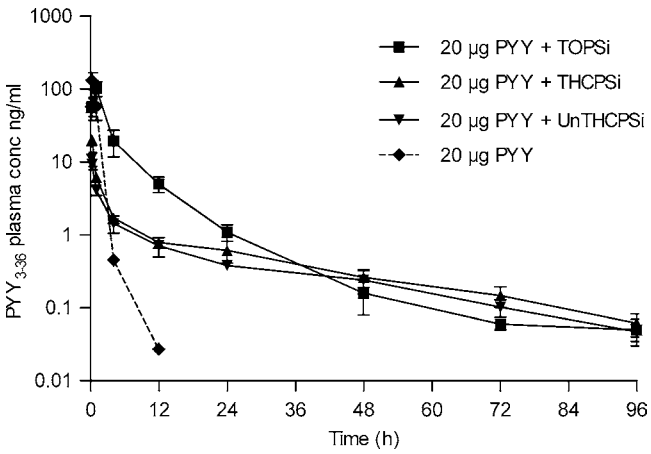

Fig. 3 Sustained PYY3-36 release after delivery in PSi microparticles is affected by surface chemistry of the microparticles (THCPSi and UnTHCPSi $n=6$, TOPSi $n=5$, PYY3-36 solution s.c. $n=4$, mean±SEM). *TOPSi *vs.* THCPSi/UnTHCPSi $p<0.001$ 0–1 h; $p<0.005$ TOPSi *vs.* THCPSi/UnTHCPSi at 4h.

DISCUSSION

The experimental protocol and the results are summarized in Fig. 4. In general, the drug molecules are adsorbed non-covalently onto PSi and released from the surface and the pores by simple diffusion as PSi wetted by the solvent or when PSi dissolves (14,42,43). The structure of the pore wall surface and the functional groups of the drug affect the adsorption interactions (4,5). Here, the investigated THCPSi, UnTHCPSi and TOPSi microparticles had comparable porous properties, *i.e.* specific surface area, pore diameter and pore volume, and PYY3-36 loading degree (12–16% w/w) as presented in Table I. Therefore, the effect of porous properties of the investigated PSi microparticles on PYY3-36 release can be excluded and the results are explained by the surface chemistry of PSi. Previously, effect of PSi surface chemistry on *in vitro* release of a protein (papain) from PSi powders was demonstrated (8). In the present study, three PSi surfaces were characterized for *in vitro* and *in vivo* peptide (PYY3-36) delivery; TOPSi surface is the most hydrophilic, whereas UnTHCPSi is moderately hydrophilic and THCPSi is hydrophobic.

The ATR-FTIR analysis of the loaded TOPSi, THCPSi and UnTHCPSi do not indicate strong interactions between the PSi surface and the loaded PYY3-36. Instead, the negligible differences observed with TOPSi may indicate that combined with the better wettability of the material, the peptide is readily desorbed from the surface, while with more hydrophobic THCPSi and UnTHCPSi PYY3-36 may be oriented towards the surface of the PSi according to its hydrophobic segments. The carboxylic acid terminated UnTHCPSi surface additionally indicates slightly stronger conformational changes than THCPSi, as the α-helix structure and random conformation related peaks at 1654 cm^{-1} and 1641 cm^{-1} become more pronounced (44). The presence of possible hydrogen bonding between the surface carboxyl groups and the peptide amine groups cannot be excluded, as both the amide I band and the adjacent carbonyl peak at 1715 cm^{-1} overlap considerably.

Table II Pharmacokinetic Values of PYY3-36 (Dose 20 μg) after Subcutaneous (s.c.) and Intravenous (i.v.) Administration in Mice. PYY3-36 was Delivered in Solutions (i.v., s.c.) and in Mesoporous Silicon (PSi) Microparticles (s.c.) with Different Surface Chemistries; Thermally Oxidized (TOPSi), Thermally Hydrocarbonized (THCPSi) and Thermally Functionalized THCPSi with Undecylenic Acid (UnTHCPSi). (Mean ± SEM, $n = 4–6$)

	PYY sol i.v.	PYY sol s.c.	TOPSi s.c.	THCPSi s.c.	UnTHCPSi s.c.
C_{max} (ng/ml)	2327 ± 725	137 ± 35[c]	103 ± 8[a,b]	22 ± 6[a,b,c]	13 ± 2[a,c]
t_{max} (min)	3 ± 1	26 ± 11	51 ± 9[d]	11 ± 2[d]	19 ± 8[d]
$t_{½}$ (h)	0.4 ±0.02	0.4 ± 0.02[c,d]	7 ± 1[a,d]	20 ± 1[a,c]	21 ± 2[a,c]
$AUC_{0\text{-last}}$ (h ng/ml)	471 ± 75	181 ± 31[a]	457 ± 73[a]	59 ± 5[a]	44 ± 5[a]
$AUC_{0\text{-}\infty}$ (h ng/ml)	471 ± 75	181 ± 31[a]	462 ± 73[a]	61 ± 6[a]	45 ± 5[a]
F(%)		38 ± 7[a]	98 ± 16[a]	13 ±2[a]	9 ± 1[a]
$F_{relative,\ s.c.}$(%)			256 ± 41[a]	34 ± 3[a]	25 ± 2[a]

[a] $p < 0.001$ TOPSi *vs*. THCPSi/UnTHCPSi/S.c. solution

[b] $p < 0.01$ TOPSi *vs* THCPSi

[c] $p < 0.001$ S.c. solution *vs* THCPSi/UnTHCPSi

[d] $p < 0.05$ TOPSi *vs* THCPSi/UnTHCPSi/S.c. solution

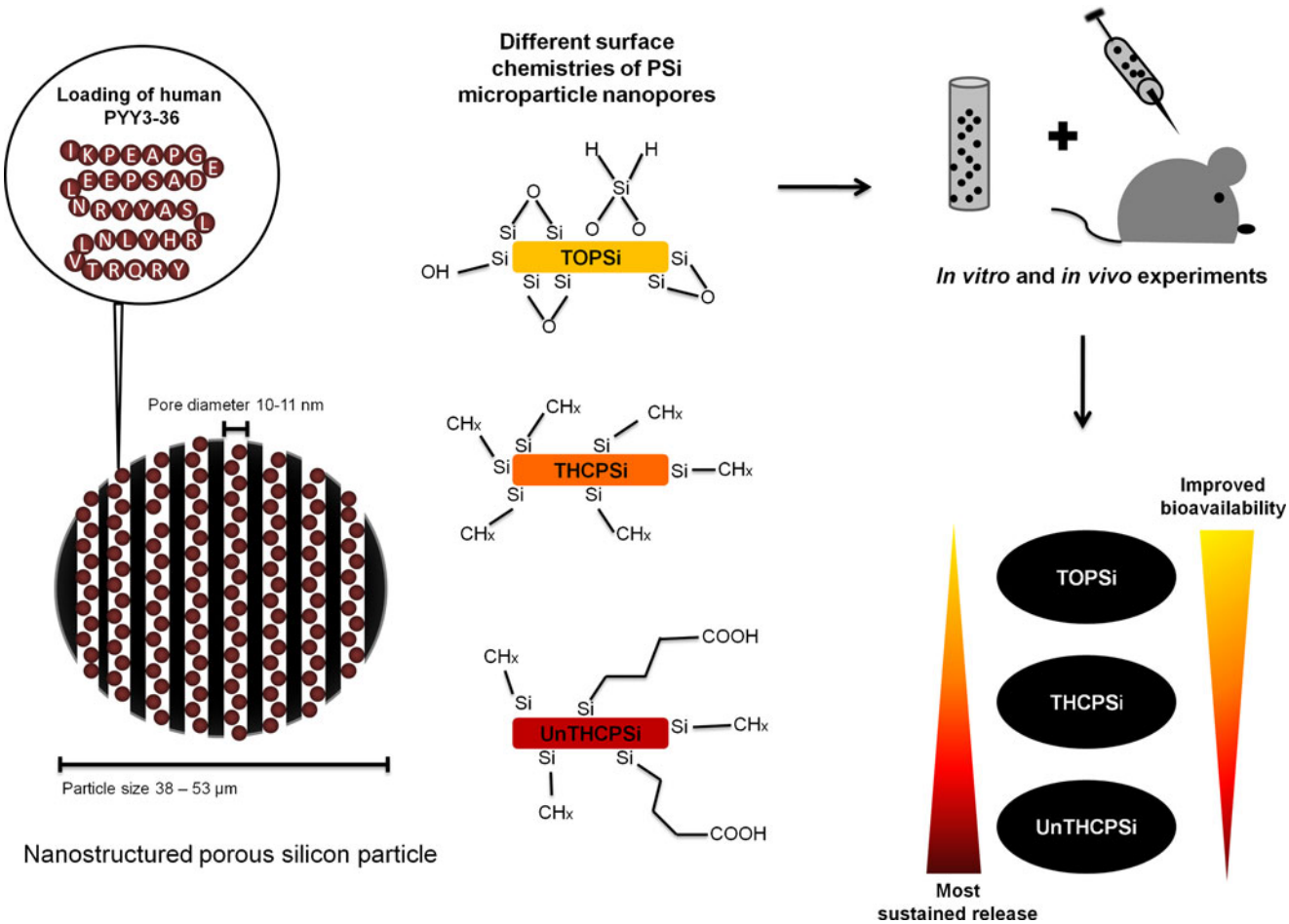

Fig. 4 Peptide YY (PYY3-36) was loaded into the nanopores of porous silicon microparticles with three different surface chemistries. The formulations were investigated both *in vitro* and *in vivo*. The surface characteristics clearly influence the PYY3-36 delivery. TOPSi improves the relative bioavailability and UnTHCPSi shows the most sustained release.

Surface chemistry of PSi clearly affected *in vitro* (Fig. 2) and *in vivo* release of PYY3-36 (Table II). Both *in vitro* and *in vivo* results indicate that TOPSi released PYY3-36 most efficiently but the absorbed fraction of PYY3-36 was higher *in vivo* than the released fraction *in vitro*. These results demonstrate the importance of both surface chemistry and release medium in the release of PYY3-36 from PSi. The interactions between PYY3-36 and PSi surface control the peptide release, which is further affected by compounds present in the release medium that may influence diffusion-controlled peptide release or dissolution rate of PSi. As mentioned earlier, in addition to the diffusion, the drug release can take place as the PSi degrades as was shown by doxorubicin release from oxidized PSi nanoparticles during their dissolution (42). Of the PSi microparticles investigated here, the degradation rate of TOPSi is the fastest while THCPSi is the most stabile. The faster degradation of TOPSi could partially explain the differences seen in the bioavailabilities values (98±16, 9±1 and 13±2%, respectively). To illustrate the complexity between the PSi *in vitro* and *in vivo* results, it was recently shown that PSi degrades faster in serum, than in phosphate buffered saline (PBS) (45), supporting our observations of significantly faster *in vivo* degradation of THCPSi (unpublished data). Therefore, the PSi degradation might not affect significantly the peptide release *in vitro* in the time frame of the experiment (14 days), but it may play a role *in vivo*. In addition, more hydrophobic particle surface of THCPSi and UnTHCPSi decreases their wetting which might slow down the peptide release.

Recently, interactions of three proteins, HSA, lysozyme and papain with TOPSi microparticles were investigated *in vitro* and TOPSi was shown to be able to preserve the native structure of the proteins and therefore the investigated proteins were suggested to maintain their biological activity (46). In addition, a recent study regarding the adsorption of lysozyme on silica nanoparticles indicated that even the conformation of a peptide may change due to the adsorption, these changes are reversed during desorption (47). The method used in the present study, for detecting PYY3-36 from plasma (ELISA), is based on specific antibody binding to active human PYY. Therefore, the assay confirms the activity of the delivered peptide. In the present study, PYY3-36 loading into PSi microparticles protected PYY3-36 from degradation before its release from the particles, since the peptide could be detected during several days from the blood circulation. The interesting result is that the TOPSi microparticles significantly improved the absolute bioavailability of PYY3-36 (98±16%) from that of the s.c. solution (38±7.5%). These results suggest that a complete absorption of subcutaneous PYY3-36 requires a tailored controlled release formulation instead of an immediate release formulation, such as solution. Also a permeation enhancing feature of PSi could also account for improved bioavailability since PSi has been reported to improve the *in vitro* permeation of furosemide (48) and insulin through Caco2-monolayers (11). However, it must be noted that, despite the promising earlier and present results, TOPSi might not be optimal for all peptides and proteins, because it is more reactive than more hydrophobic PSi surfaces. In addition, further studies are needed to clarify the mechanism of subcutaneous PYY3-36 absorption.

CONCLUSION

This work demonstrates that PSi microparticles are capable to achieve a high a peptide loading degree and sustained *in vivo* PYY3-36 delivery over several days. In addition, the peptide releasing properties can be modified with different surface chemistries and therefore the release can be optimized as needed for the particular peptide. In the case of PYY3-36, TOPSi microparticles are capable of significantly improving the absolute bioavailability when compared with subcutaneous administration of PYY3-36 solution.

ACKNOWLEDGMENTS & DISCLOSURES

This study was financially supported by Finnish Cultural Foundation (MK), Orion Farmos Research Foundation (MK), Graduate School of Pharmaceutical Research (JM), Academy of Finland – PEPBI consortium (#117906, #118002, #217547) and the strategic funding of the University of Eastern Finland (NAMBER consortium).

REFERENCES

1. Salonen J, Kaukonen AM, Hirvonen J, Lehto VP. Mesoporous silicon in drug delivery applications. J Pharm Sci. 2008;97:632–53.
2. Bimbo LM, Sarparanta M, Santos HA, Airaksinen AJ, Mäkilä E, Laaksonen T, *et al.* Biocompatibility of thermally hydrocarbonized porous silicon nanoparticles and their biodistribution in rats. ACS Nano. 2010;4:3023–32.
3. Tanaka T, Godin B, Bhavane R, Nieves-Alicea R, Gu J, Liu X, *et al. In vivo* evaluation of safety of nanoporous silicon carriers following single and multiple dose intravenous administrations in mice. Int J Pharm. 2010;402:190–7.
4. Limnell T, Riikonen J, Salonen J, Kaukonen AM, Laitinen L, Hirvonen J, *et al.* Surface chemistry and pore size affect carrier properties of mesoporous silicon microparticles. Int J Pharm. 2007;343:141–7.
5. Salonen J, Laitinen L, Kaukonen AM, Tuura J, Björkqvist M, Heikkilä T, *et al.* Mesoporous silicon microparticles for oral drug

delivery: loading and release of five model drugs. J Control Release. 2005;108:362–74.
6. Karlsson LM, Tengvall P, Lundström I, Arwin H. Penetration and loading of human serum albumin in porous silicon layers with different pore sizes and thicknesses. J Colloid Interface Sci. 2003;266:40–7.
7. Prestidge CA, Barnes TJ, Mierczynska-Vasilev A, Kempson I, Peddie F, Barnett C. Peptide and protein loading into porous silicon wafers. Phys Stat Sol (a). 2008;205:311–5.
8. Prestidge CA, Barnes TJ, Mierczynska-Vasilev A, Skinner W, Peddie F, Barnett C. Loading and release of a model protein from porous silicon powders. Phys Stat Sol (a). 2007;204:3361–6.
9. Wang F, Hui H, Barnes TJ, Barnett C, Prestidge CA. Oxidized mesoporous silicon microparticles for improved oral delivery of poorly soluble drugs. Mol Pharm. 2010;7:227–36.
10. Wu EC, Park JH, Park J, Segal E, Cunin F, Sailor MJ. Oxidation-triggered release of fluorescent molecules or drugs from mesoporous Si microparticles. ACS Nano. 2008;2:2401–9.
11. Foraker AB, Walczak RJ, Cohen MH, Boiarski TA, Grove CF, Swaan PW. Microfabricated porous silicon particles enhance paracellular delivery of insulin across intestinal Caco-2 cell monolayers. Pharm Res. 2003;20:110–6.
12. De Rosa E, Chiappini C, Fan D, Liu X, Ferrari M, Tasciotti E. Agarose surface coating influences intracellular accumulation and enhances payload stability of a nano-delivery system. Pharm Res. 2011;28:1520–30.
13. Kilpeläinen M, Riikonen J, Vlasova MA, Huotari A, Lehto VP, Salonen J, *et al. In vivo* delivery of a peptide, ghrelin antagonist, with mesoporous silicon microparticles. J Control Release. 2009;137:166–70.
14. Kilpeläinen M, Mönkäre J, Vlasova MA, Riikonen J, Lehto VP, Salonen J, *et al.* Nanostructured porous silicon microparticles enable sustained peptide (Melanotan II) delivery. Eur J Pharm Biopharm. 2011;77:20–5.
15. Frokjaer S, Otzen DE. Protein drug stability: a formulation challenge. Nat Rev Drug Discov. 2005;4:298–306.
16. Witschi C, Doelker E. Peptide degradation during preparation and *in vitro* release testing of poly(L-lactic acid) and poly(DL-lactic-co-glycolic acid) microparticles. Int J Pharm. 1998;171:1–18.
17. Ye M, Kim S, Park K. Issues in long-term protein delivery using biodegradable microparticles. J Control Release. 2010;146:241–60.
18. Salonen J, Björkqvist M, Laine E, Niinistö L. Stabilization of porous silicon surface by thermal decomposition of acetylene. App Surf Science. 2004;225:389–94.
19. Karhunen LJ, Juvonen KR, Huotari A, Purhonen AK, Herzig KH. Effect of protein, fat, carbohydrate and fibre on gastrointestinal peptide release in humans. Regul Pept. 2008;149:70–8.
20. Tatemoto K, Mutt V. Isolation of two novel candidate hormones using a chemical method for finding naturally occurring polypeptides. Nature. 1980;285:417–8.
21. Nonaka N, Shioda S, Niehoff ML, Banks WA. Characterization of blood–brain barrier permeability to PYY3-36 in the mouse. J Pharmacol Exp Ther. 2003;306:948–53.
22. Koegler FH, Enriori PJ, Billes SK, Takahashi DL, Martin MS, Clark RL, *et al.* Peptide YY(3–36) inhibits morning, but not evening, food intake and decreases body weight in rhesus macaques. Diabetes. 2005;54:3198–204.
23. Beglinger C, Poller B, Arbit E, Ganzoni C, Gass S, Gomez-Orellana I, *et al.* Pharmacokinetics and pharmacodynamic effects of oral GLP-1 and PYY3-36: a proof-of-concept study in healthy subjects. Clin Pharmacol Ther. 2008;84:468–74.
24. Chelikani PK, Haver AC, Reeve Jr JR, Keire DA, Reidelberger RD. Daily, intermittent intravenous infusion of peptide YY(3–36) reduces daily food intake and adiposity in rats. Am J Physiol Regul Integr Comp Physiol. 2006;290:R298–305.
25. Batterham RL, Cowley MA, Small CJ, Herzog H, Cohen MA, Dakin CL, *et al.* Gut hormone PYY(3–36) physiologically inhibits food intake. Nature. 2002;418:650–4.
26. Batterham RL, Cohen MA, Ellis SM, Le Roux CW, Withers DJ, Frost GS, *et al.* Inhibition of food intake in obese subjects by peptide YY3-36. N Engl J Med. 2003;349:941–8.
27. Abbott CR, Small CJ, Kennedy AR, Neary NM, Sajedi A, Ghatei MA, *et al.* Blockade of the neuropeptide Y Y2 receptor with the specific antagonist BIIE0246 attenuates the effect of endogenous and exogenous peptide YY(3–36) on food intake. Brain Res. 2005;1043:139–44.
28. van den Hoek AM, Heijboer AC, Voshol PJ, Havekes LM, Romijn JA, Corssmit EP, *et al.* Chronic PYY3-36 treatment promotes fat oxidation and ameliorates insulin resistance in C57BL6 mice. Am J Physiol Endocrinol Metab. 2007;292:E238–45.
29. Karra E, Chandarana K, Batterham RL. The role of peptide YY in appetite regulation and obesity. J Physiol. 2009;587:19–25.
30. Chandarana K, Batterham R, Peptide YY. Curr Opin Endocrinol Diabetes Obes. 2008;15:65–72.
31. Karra E, Batterham RL. The role of gut hormones in the regulation of body weight and energy homeostasis. Mol Cell Endocrinol. 2010;316:120–8.
32. Shechter Y, Tsubery H, Mironchik M, Rubinstein M, Fridkin M. Reversible PEGylation of peptide YY3-36 prolongs its inhibition of food intake in mice. FEBS Lett. 2005;579:2439–44.
33. Gantz I, Erondu N, Mallick M, Musser B, Krishna R, Tanaka WK, *et al.* Efficacy and safety of intranasal peptide YY3-36 for weight reduction in obese adults. J Clin Endocrinol Metab. 2007;92:1754–7.
34. A Study of Nasal PYY3-36 and Placebo for Weight Loss in Obese Subjects. ClinicalTrials.Gov. 2011 June 10. Available from: http://clinicaltrials.gov/ct2/show/NCT00537420).
35. Akers JM, DeFelippis RM. Peptides. In: Frokjaer S, Hovgaard L, editors. Pharmaceutical formulation development of peptides and proteins. London: CRC; 1999. p. 145–77.
36. Boukherroub R, Wojtyk JTC, Wayner DDM, Lockwood DJ. Thermal hydrosilylation of undecylenic acid with porous silicon. J Electrochem Soc. 2002;149:H59–63.
37. Brunauer S, Emmett P, Teller E. Adsorption of gases in multimolecular layers. J Am Chem Soc. 1938;60:309–19.
38. Barrett EP, Joyner LG, Halenda PP. The determination of pore volume and area distributions in porous substances. I. Computations from nitrogen isotherms. J Am Chem Soc. 1951;73:373–80.
39. Lehto VP, Vähä-Heikkilä K, Paski J, Salonen J. Use of thermoanalytical methods in quantification of drug load in mesoporous silicon microparticles. J Therm Anal Calorimetry. 2005;80:393–7.
40. Arrondo JL, Goni FM. Structure and dynamics of membrane proteins as studied by infrared spectroscopy. Prog Biophys Mol Biol. 1999;72:367–405.
41. Boxenbaum H. Pharmacokinetics tricks and traps: flip-flop models. J Pharm Pharm Sci. 1998;1:90–1.
42. Park JH, Gu L, von Maltzahn G, Ruoslahti E, Bhatia SN, Sailor MJ. Biodegradable luminescent porous silicon nanoparticles for *in vivo* applications. Nat Mater. 2009;8:331–6.
43. Leoni L, Boiarski A, Desai TA. Characterization of nanoporous membranes for immunoisolation: Diffusion properties and tissue effects. Biomed Microdevices. 2002;4:131–9.
44. Hegefeld WA, Kuczera K, Jas GS. Structural dynamics of neuropeptide hPYY. Biopolymers. 2011;95:487–502.

45. Godin B, Gu J, Serda RE, Bhavane R, Tasciotti E, Chiappini C, *et al.* Tailoring the degradation kinetics of mesoporous silicon structures through PEGylation. J Biomed Mater Res Part A. 2010;94A:1236–43.
46. Jarvis KL, Barnes TJ, Prestidge CA. Thermal oxidation for controlling protein interactions with porous silicon. Langmuir: the ACS journal of surfaces and colloids. 2010;26:14316–22.
47. Felsovalyi F, Mangiagalli P, Bureau C, Kumar SK, Banta S (2011) Reversibility of the adsorption of lysozyme on silica. Langmuir; doi:10.1021/la202585r.
48. Kaukonen AM, Laitinen L, Salonen J, Tuura J, Heikkilä T, Limnell T, *et al.* Enhanced *in vitro* permeation of furosemide loaded into thermally carbonized mesoporous silicon (TCPSi) microparticles. Eur J Pharm Biopharm. 2007;66:348–56.